# An Immunoglobulin Superfamily-Like Domain Unique to the *Yersinia pseudotuberculosis* Invasin Protein Is Required for Stimulation of Bacterial Uptake via Integrin Receptors

PETRA DERSCH[1,2] AND RALPH R. ISBERG[1,3]*

*Department of Molecular Biology and Microbiology, Tufts University School of Medicine,[1] and Howard Hughes Medical Institute,[3] Boston, Massachusetts 02111, and Institute of Microbiology, Freie Universität, 14195 Berlin, Germany[2]*

The binding of the *Yersinia pseudotuberculosis* and *Yersinia enterocolitica* invasin proteins to $\beta_1$ integrin receptors allows internalization of these organisms by cultured cells. The C-terminal 192-residue superdomain of the *Y. pseudotuberculosis* invasin is necessary and sufficient for integrin recognition, while a region located outside, and N-terminal to, this superdomain strongly enhances the efficiency of bacterial uptake. Within the enhancer region is a domain called D2 that allows invasin-invasin interaction. To investigate the role of the enhancer region, bacterial cell binding and entry mediated by the *Y. pseudotuberculosis* invasin protein (invasin$_{pstb}$) was compared to that of *Y. enterocolitica* invasin (invasin$_{ent}$), which lacks the D2 self-association domain. Invasin$_{ent}$ was shown to be unable to promote self-interaction, using the DNA binding domain of $\lambda$ repressor as a reporter. Furthermore, two genetically engineered in-frame deletion mutations that removed D2 from invasin$_{pstb}$ were significantly less proficient than wild-type invasin$_{pstb}$ at promoting uptake, although the amount of surface-exposed invasin as well as the cell binding capacity of the recombinant *Escherichia coli* strains remained similar. Competitive uptake assays showed that *E. coli* cells expressing invasin$_{pstb}$ had a significant advantage in the internalization process versus either *E. coli* cells expressing invasin$_{ent}$ or the invasin$_{pstb}$ derivatives deleted for D2, further demonstrating the importance of invasin self-interaction for the efficiency of invasin-mediated uptake.

Many bacterial pathogens have adopted strategies to adhere to and efficiently penetrate normally nonphagocytic host cells (3, 8, 15). Entry into host cells permits bacteria to either grow and multiply in a protected niche (30) or to gain access to other tissues within the host (11, 30). The latter tactic is used by a number of enteric pathogens that translocate into subepithelial sites, allowing the initiation of systemic disease. A favored cell type for the spread of pathogens from the intestine is the M cell, which can be found interdigitated within the epithelium overlying lymphoid Peyer's patches in the small intestine (31). In the case of enteropathogenic *Yersinia* organisms, the tropism for this cell type can partly be explained by the fact that no other cell in the intestinal epithelium efficiently presents the receptors that recognize the bacterial invasin protein, which is required for efficient translocation into Peyer's patches (25, 31, 33).

Invasin is encoded by both *Yersinia enterocolitica* and *Yersinia pseudotuberculosis* and apparently plays a similar role in both organisms, allowing bacterial colonization of regional lymph nodes after ingestion (25, 33). The protein is localized in the outer membrane, with the C-terminal 479 amino acids of the *Y. pseudotuberculosis* invasin protein (invasin$_{pstb}$) exposed on the bacterial cell surface (22, 23). This region is responsible for promoting cell adhesion and uptake by binding to multiple $\beta$-chain integrin receptors on the host eukaryotic cell (16). The N-terminal half of invasin appears to be required for export of

the hydrophilic C-terminal region across the outer membrane (22).

The integrin receptor family consists of several related heterodimeric integral membrane proteins, involved in various adhesive functions, including cell-cell interaction, cell migration, cellular differentiation, and attachment to extracellular matrix proteins (14). Integrin receptors, via their cytoplasmic domains, are capable of signaling to cytoskeletal components after adhering to substrates. Invasin-mediated bacterial uptake is inhibited by drugs that antagonize either actin polymerization or tyrosine phosphorylation (9, 36). One tyrosine-phosphorylated mammalian protein that is clearly required for uptake is FAK (1). In addition, determinants within the cytoplasmic domain of the integrin that allow association of the receptor with the cytoskeleton and endocytic components modulate the efficiency of bacterial uptake (41).

The crystal structure of the C terminus of *Y. pseudotuberculosis* invasin has been determined, extending from residues 503 to 986 (12). The protein is arrayed as a series of five domains, extending in a rod-like 180-Å structure (see Fig. 1A). The first four domains (D1 to D4) are predominantly $\beta$ stranded, each adopting a folding topology found in members of the immunoglobulin superfamily. The fifth domain (D5), which has interspersed $\alpha$-helical and $\beta$-stranded regions, is related to C-type lectin-like domains (42). The minimal region of invasin required for binding to integrin receptors contains just D4 and D5 (22). D4 and D5 have a large interdomain interface, resulting in the formation of a superdomain extending from residues 795 to 986. Residues from both D4 and D5 appear to be presented to the integrin receptor, because point mutations in both domains result in defective receptor binding (24, 37). A derivative containing just D4 and D5, when coated as a monomer on the surface of latex bead, is inefficient at promoting

* Corresponding author. Mailing address: Department of Molecular Biology & Microbiology, Tufts University School of Medicine, Howard Hughes Medical Institute, 136 Harrison Ave., Boston, MA 02111. Phone: (617) 636-3993. Fax: (617) 636-0337. E-mail: risberg@opal .tufts.edu.
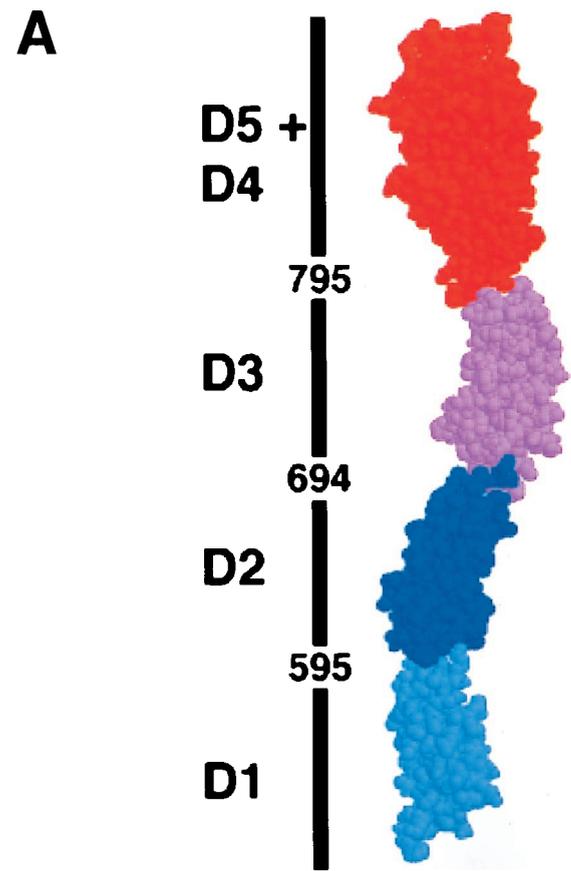
FIG. 1. (A) Spacefilling representation of the invasin$_{pstb}$ crystal structure. Different domains are indicated as D1 through D5 and depicted as different colors. Residue numbers that are located in interdomain regions are noted next to the structure. The region sufficient to promote cI multimerization is shown in dark blue and represents the entire D2 region in the crystal structure. The minimal region necessary for integrin recognition is shown in red and is the D4-D5 superdomain (12). (B) Comparison of a portion of *Y. pseudotuberculosis* invasin sequence and selected orthologs from other gram-negative bacteria. The predicted amino acid sequence (amino acids 555 to 734) of invasin$_{pstb}$ (19), extending from the middle of D1 to the middle of D3, is shown in panel A. This is aligned with the sequences of *Y. enterocolitica* invasin (45) and the enterohemorrhagic *E. coli* (EHEC) intimin. The *Citrobacter freundii* and enteropathogenic *E. coli* intimins align similarly to the EHEC protein (data not shown). The amino acid sequences of two genetically engineered invasin$_{pstb}$ mutants cloned on plasmids pPD254 and pPD255 are shown below. Sequences were aligned by the program Clustal W (2). Residue numbers of each protein are given at the start and the end of each line. Identical amino acid residues found among all proteins are noted with asterisks (∗). Similar amino acid residues are enclosed by shaded boxes. The boxed sequence of the *Y. pseudotuberculosis* invasin represents the domain responsible for multimerization and is coincident with the endpoints of D2 in the crystal structure (12). The dashes indicate the regions that are deleted in invasin$_{ent}$ and intimins.

uptake of integrin-bound particles (7). As beads coated by D1 to D5 can be internalized efficiently, residues within D1 and D3 enhance uptake.

An activity that may play a role in enhancing uptake has been identified in D2. Hybrid proteins containing only residues from this domain are capable of promoting homotypic interaction (7). No other portion of the determined structure is capable of this activity. That invasin self-interaction appears to play a role in uptake is supported by the fact that beads coated with D4 and D5 are internalized if this superdomain is dimerized by binding to immunoglobulin G-coated particles (7).

The ability of invasin$_{pstb}$ D2 to self-associate and the importance of D1 to D3 in promoting efficient uptake has led to the proposal that direct interaction of multimeric invasin with mul-

tiple integrins mediates receptor clustering, resulting in an intracellular signal for bacterial uptake (7). The *Y. enterocolitica* invasin protein (invasin$_{ent}$), which exhibits an overall homology of 85% to invasin$_{pstb}$, has an internal deletion of 99 amino acids that completely removes D2 (Fig. 1B) (45). Several sequence comparison programs place a similar deletion within the intimins, bacterial cell attachment proteins that have high sequence similarity to invasin (10, 20, 39). The recently described global fold of the carboxyl-terminal 280-amino-acid fragment of one such intimin is highly similar to the folding pattern of invasin domains D3 to D5, emphasizing that these proteins are part of a single family (21, 26). Even so, intimins are able to mediate bacterial adhesion to host cells in the absence of a homologous D2 region.

TABLE 1. Bacterial strains, plasmids, and bacteriophages

| Strains, plasmids, and phage | Description[a] | Reference |
|---|---|---|
| **Strains** | | |
| *E. coli* K12 | | |
| XL1blue | F′::Tn*10 proA*$^+$*B*$^+$ *lacI*$^q$ Δ(*lacZ*)M15/*recA1 endA1 gyrA96* (Nal$^r$) *thi hsdR17* (r$_K$$^-$ m$_K$$^+$) *supE44 relA1 lac* | 6 |
| JH372 | lysogenic λ202 (*imm* 21 P$_R$-*lacZ* ΔO$_{R2}$) | 13 |
| SR2 | F$^-$ *araD* Δ(*lacU*) Δ*phoA lpp5508 galE rpsL galE galK degP*::Tn*5* | 35 |
| *Y. pseudotuberculosis* | Type III(P$^+$), pIB1 | 4 |
| *Y. enterocolitica* 8081 c | | 32 |
| **Plasmids** | | |
| pBR322 | Cloning vector, Ap$^r$ | 5 |
| pHSG575/576 | pSC101-based cloning vectors, p*lacZ* MCS, *lacZ*′, Cm$^r$ | 40 |
| pMin3 | Produces MBP-Inv$_{ent}$ fusion protein, Ap$^r$ | 32 |
| pFG157 | λ *c*I *ind1*, *lacUV5* promoter, colE1, *ori*, Ap$^r$ | 13 |
| pJH370 | λ *c*I *ind1* aa 1–132 fused to zipper domain of GCN4, Ap$^r$ | 13 |
| pJH391 | λ *c*I *ind1* aa 1–132 fused to *lacZ*, Ap$^r$ | 13 |
| pKH101 | λ *c*I *ind1* aa 1–132[b] Ap$^r$ | 13 |
| pPD207 | pHSG576, *inv*$_{pstb}$$^+$, Ap$^r$ | This work |
| pPD208 | Produces cI$_N$-Inv509-986-Inv$_{pstb}$478,[b] Ap$^r$ | 7 |
| pPD210 | Produces cI$_N$-Inv795-986-Inv$_{pstb}$202,[b] Ap$^r$ | 7 |
| pPD226 | Produces cI$_N$-Inv575-694,[b] Ap$^r$ | 7 |
| pPD229 | Produces cI$_N$-Inv$_{ent}$456-835,[b] Ap$^r$ | This work |
| pPD230 | Produces cI$_N$-Inv$_{pstb}$575-694-Inv$_{ent}$456-835,[b] Ap$^r$ | This work |
| pPD231 | pHSG576 *inv*$_{ent}$$^+$, Cm$^r$ | This work |
| pPD244 | Produces cI$_N$-Inv596-694-Inv$_{ent}$380,[b] Ap$^r$ | 7 |
| pPD254 | pPD207, *inv*$_{pstb}$(Δ1-595-697),[c] Cm$^r$ | This work |
| pPD255 | pPD207, *inv*$_{pstb}$(Δ2-594-697),[d] Cm$^r$ | This work |
| pPD256 | pPD207, Ap$^r$, Cm$^s$ | This work |
| pRI203 | pBR325 *inv*$^+$, Ap$^r$ | 19 |
| pRI253 | pT7-4 *inv*$^+$, Ap$^r$ | 18 |
| pRI285 | Produces MBP-Inv497$_{pstb}$ fusion protein | 24 |
| pZ150 | Cloning vector carrying *lacUV5* promoter, Ap$^r$ | 13 |
| **Bacteriophage** | | |
| λKH54 | Δ*c*I | 13 |

[a] aa, amino acid; Ap$^r$, ampicillin resistance; Cm$^r$, chloramphenicol resistance; Cm$^s$, chloramphenicol sensitivity; Nal$^r$, nalidixic acid resistance.
[b] Protein expressed from the *lacUV5* promoter; the numbers of the range indicate the amino acids of *inv*$_{pstb}$ fused to cI$_N$′.
[c] The numbers indicate the amino acids of *inv*$_{pstb}$ deleted in the construct.
[d] The numbers indicate the amino acids of *inv*$_{pstb}$ deleted in the construct; in addition, amino acids AVLP from the equivalent *Y. enterocolitica* sequence were introduced into this region (see Fig. 1).

In this study, the activities of invasin derivatives lacking D2 were examined. The lack of this domain in the wild-type invasin$_{ent}$ protein was found to lower the efficiency of bacterial internalization relative to invasin$_{pstb}$ and eliminate efficient homotypic interaction. This difference in the activity of the two proteins may contribute to the observed differences in the colonization pattern of these two organisms within intestinal lymph nodes, as *Y. enterocolitica* efficiently proliferates and forms large abscesses in these sites, whereas *Y. pseudotuberculosis* does not.

## MATERIALS AND METHODS

**Bacterial strains, cell culture, and media.** Bacterial strains, phages, and plasmids used in this study are described in Table 1. Bacterial strains were grown with aeration in Luria-Bertani broth (Difco) or in M9 medium containing 0.4% glucose (27, 38) at 37°C (*Escherichia coli*) or at 28°C (*Yersinia*). The antibiotics used for bacterial selection were as follows: ampicillin, 100 μg/ml; chloramphenicol, 30 μg/ml; tetracycline, 5 μg/ml; kanamycin, 50 μg/ml; gentamicin, 50 μg/ml. HEp-2 cells were cultured in RPMI 1640 media (Irvine Scientific) supplemented with 5% newborn calf serum (Life Technology Inc.) and 2 mM glutamine at 37°C in the presence of 5% $CO_2$.

**Nucleic acid techniques.** Preparations of small-scale plasmid DNA, restriction digestions, ligations, and transformations were performed as previously described (27, 38). Large-scale plasmid preparations were purified on Qiagen columns (Hilden, Germany) according to manufacturer's protocols. PCR products were purified with the QIAquick Kit (Qiagen) before and after restriction digestions.

PCRs were performed in a 100-μl mixture consisting of 1× *Taq* polymerase buffer, 0.2 mM concentration of deoxynucleoside triphosphate (Pharmacia Biotech), 10 pmol of each primer, 0.5 μg of template DNA, 5 mM MgCl₂, and 2.5 U of recombinant *Taq* polymerase (Perkin-Elmer Cetus). The reactions were performed as follows: denaturation at 95°C for 5 min, 20 cycles annealing at 58°C for 30 s, extension at 72°C for 30 s to 2 min (depending on the length of the expected PCR product), and 95°C for 30 s, in a DNA thermal cycler PTC-200 (MJ Research).

**Plasmids and oligonucleotides.** Plasmids used in this study are listed in Table 1. Plasmid pPD207 (*inv*$_{pstb}$$^+$) was derived by inserting the *Eco*RI-*Hin*dIII fragment of pRI253 (17), carrying the entire *inv*$_{pstb}$ gene into the *Eco*RI and *Hin*dIII sites of pHSG576 (40). Plasmid pPD231 (*inv*$_{ent}$$^+$) was constructed by inserting a PCR fragment harboring the *inv*$_{ent}$ gene, including the *inv*$_{ent}$ promoter, into vector pHSG575 that was cut with *Eco*RI and *Bam*HI. This product was generated by using the upstream primer *inv*$_{ent}$ (5′-CCATAT<u>GAATTC</u>CTTAACTAAGCCAGCGGTTGC-3′) (creates an *Eco*RI site) and downstream primer *inv*$_{ent}$ (5′-AACGGT<u>GGATCCC</u>CGGCAACCTGCATAACGGGC-3′) (creates a *Bam*HI site). The in-frame deletion derivatives of *inv*$_{pstb}$ that mimic the *inv* sequence of *Y. enterocolitica* were constructed by using the Transformer site-
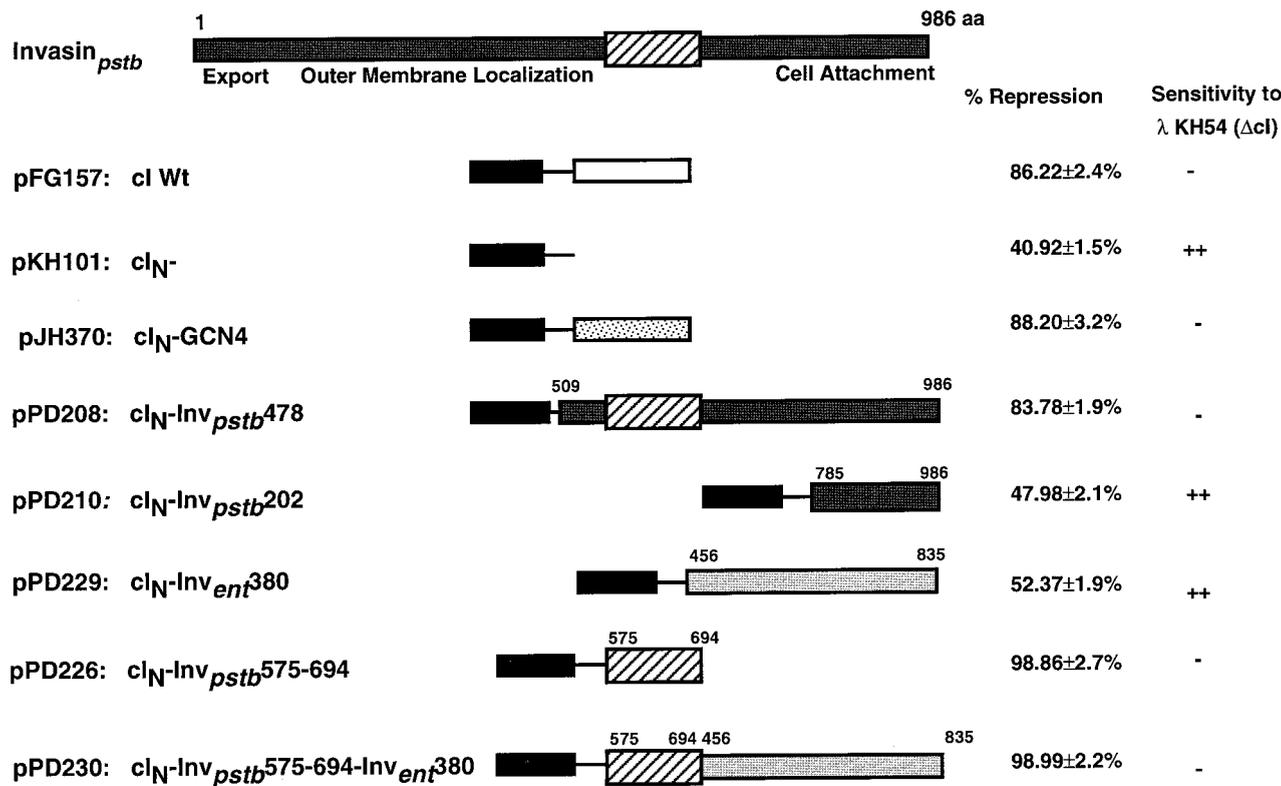
FIG. 2. Repressor activity of cI$_N$-Inv chimeric proteins. Schematic representations of invasin and the chimeric cI$_N$-Inv proteins are shown. The cI$_N$ portion of the chimeric proteins (DNA binding domain) is shown as a black box, and the dimerization domain of λ repressor is shown as white box. The invasin sequence of *Y. pseudotuberculosis* is represented by dark gray boxes, with the exception of the region encoding domain 2, which is cross-hatched. The sequences of *Y. enterocolitica* are shown as light gray boxes, which are aligned in relationship to the invasin wild-type sequence. Repression activity of the chimera and sensitivity to phage KH54(ΔcI) were measured as described (see Materials and Methods). The efficiency of KH54(ΔcI) plating represents sensitivity to a phage lysate of 10$^9$ phages/ml. −, no plaque formation; +, plaque formation.

directed mutagenesis kit (Clontech). For selection, primer 5′-GGGAAAACTG TCCTGCAGCACAGATGAAAACGG-3′ (creates a *Pst*I site) was used, designed to change the unique *Nde*I site in pHSG576 into a *Pst*I site. For pPD254 and pPD255, primers 5′-GTTGATACCGACTTTGTT-Δ-CCTATTCCAGATG CTGGC-3′ and 5′-GTTGATACCGACTTT GCC GTG CTG CCG CCTATTC CAGATGCTGGC-3′ were used as mutagenic primers (Δ labels the deletion introduced in *inv*$_{pstb}$, underlined codons show the AVLP sequence introduced at the deletion site of *inv*$_{pstb}$ [Fig. 1B]). To change the antibiotic resistance of pPD207 and generate pPD256, the *bla* gene of pBR322 was amplified with primers 5′-GCGGCGCCATGGGGAAATGTGCGCGGAACC-3′ and 5′-GCG GCGCCATGGTCTGACAGTTACCAATGC-3′ (creating *Nco*I sites) and inserted into the unique *Nco*I site in the chloramphenicol resistance gene of pPD207.

To construct the chimeric cI$_N$-Inv$_{ent}$380 protein encoded by plasmid pPD229, the DNA-binding domain of cI (cI$_N$) was fused to the C-terminal 380 amino acids of invasin$_{ent}$. To this end, a fragment of the *inv* gene of *Y. enterocolitica* (*inv$_{ent}$*) encompassing amino acids 456 to 835 was amplified by PCR using upstream primer 5′-TATTACGTCGACAGTGACTGATGATGGTGCGCTTGC-3′ (creating a *Sal*I site) and downstream primer 5′-AACGGTGGATCCCGGCAACC TGCATAACGGGC-3′ (creating a *Bam*HI site) and cloned into the *Sal*I and *Bam*HI site of pJH391 encoding cI$_N$ (13). To generate cI$_N$-Inv$_{pstb}$575-694-Inv$_{ent}$380 encoded by plasmid pPD230, a PCR-derived fragment carrying invasin$_{pstb}$, codons 575 to 694, was inserted into the *Sal*I site upstream of the *inv$_{ent}$* gene on pPD229, using primers 5′-GGGGGGGTCGACGGTGATAACCACCA GTAATGGTGCG-3′ and 5′-GGGGGGGGGTCGACGGATCTGCCGTGAAA TTAACCG3′, both creating *Sal*I sites. A schematic representation of the cI$_N$-*inv* constructs is shown in Fig. 2. Oligonucleotides were synthesized by the Howard Hughes Medical Institute Microchemical Facility (Harvard Medical School, Boston, Mass.).

**Overexpression of invasin homologues.** For cell binding and cellular uptake experiments with *E. coli* cells harboring invasin derivatives, bacteria were grown in M9 medium containing 0.4% glucose and antibiotic to an absorbance at 600 nm (A$_{600}$) of 0.7. Induction of invasin expression was performed by adding 2 mM IPTG (isopropyl-β-D-thiogalactopyranoside) (Sigma) for 60 min to the growth medium. Bacteria used in cell binding assays were adjusted to the identical

densities, and viable counts were performed on each culture to determine the exact multiplicities of infection.

**Expression and purification of MBP-Inv fusion proteins.** The purification of the MBP-Inv hybrid proteins were performed as previously described (7), with slight modifications (7). One liter of *E. coli* SR2 cells carrying either plasmid pMin3 or pRI285 was grown at 28°C in L broth to an A$_{600}$ of 0.7 before adding IPTG to a final concentration of 2 mM. The cells were then grown at 28°C for 2 additional hours before being harvested, and all following procedures were performed at 4°C. Cells were resuspended in 5 ml of 10 mM Tris (pH 8.0) with a protease inhibitor cocktail containing 5 mM phenylmethylsulfonyl fluoride, 10 mM Pepstatin (Sigma), 10 mM E64 (Boehringer Mannheim), 20 μM Leupeptin (United States Biochemical), and 10 μM Chymostatin (Sigma). Subsequently, the cells were lysed by sonication (Branson Instruments; 50% pulse, 5 min). The soluble MBP-Inv protein extract was separated from insoluble cell material by centrifugation at 25,000 × g and purified by affinity chromatography on cross-linked amylose as described previously (22, 35). MBP-Inv497 was purified by ion-exchange chromatography (7, 24). Protein concentrations were determined by the bicinchoninic acid protein assay (Pierce).

**Preparation of total cell extracts, gel electrophoresis, and Western blotting.** Cultures of *E. coli* XL1blue cells harboring the various *inv* alleles on plasmids pPD207, pPD231, pPD254, and pPD255 were grown overnight at 37°C in Luria-Bertani medium. The optical density was adjusted, and a 1-ml aliquot was withdrawn from each culture. The cells were collected by centrifugation, resuspended in 100 μl of sample buffer (0.06 M Tris [pH 6.8], 2% sodium dodecyl sulfate [SDS], 10% glycerol, 3% dithiothreitol, 0.001% bromphenol blue) and subsequently lysed by incubation at 100°C for 5 min. To reduce the viscosity of the total cell extracts, 3 μl of benzon nuclease (Merck, Darmstadt, Germany) was added to the samples and incubated at 37°C for 10 min. For the immunological detection of the invasin proteins, 2-μl portions of the total cellular extracts were loaded onto SDS–10% polyacrylamide gels, and the proteins were separated by electrophoresis and transferred to an Immobilon membrane (Millipore). The bound proteins were then probed with a monoclonal invasin$_{pstb}$- or polyclonal invasin$_{ent}$-specific antiserum. The antigen-antibody complexes were visualized with a second goat alkaline-phosphatase-conjugated antibody (Sigma) using
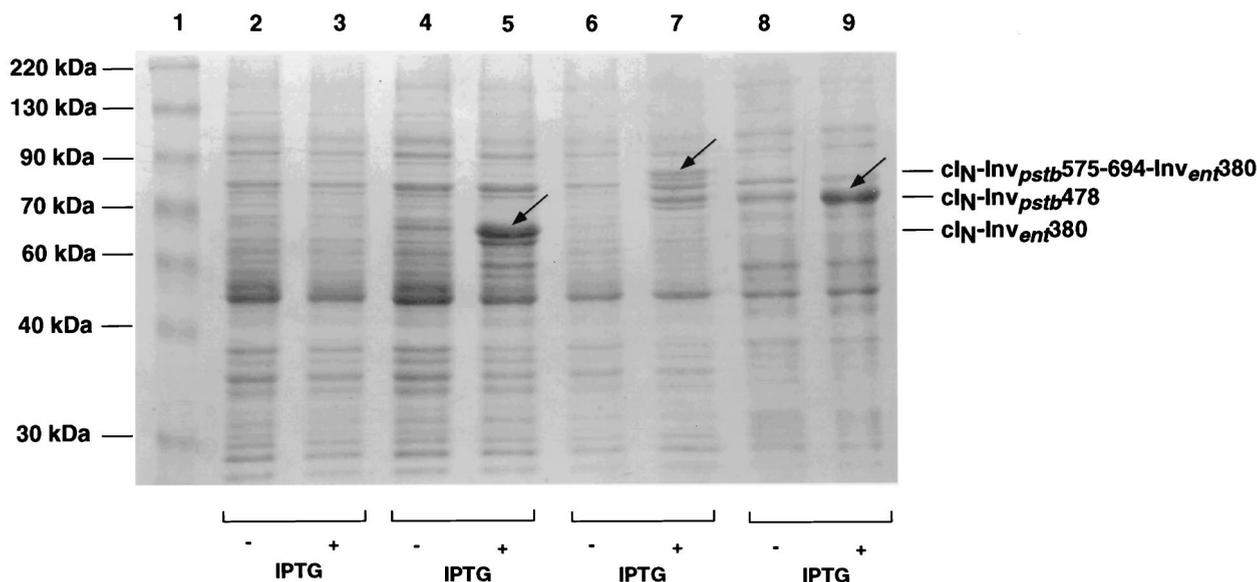
FIG. 3. Expression of the $cI_N$-$inv$ gene products of $Y.$ $pseudotuberculosis$ and $Y.$ $enterocolitica$ in $E.$ $coli$. Total cell extracts were prepared from strain JH372 carrying the $cI_N$-$inv$ fusions grown either in the presence (+IPTG) or absence (−IPTG) of inducer. The proteins were electrophoretically separated on an SDS–12% polyacrylamide gel, and the gel was stained with Coomassie brilliant blue. The arrows indicate the position of the $cI_N$-Inv hybrid proteins and a molecular mass standard is shown in lane 1. Lanes 2 and 3, JH372 pKH101; lanes 4 and 5, JH372 pPD229 ($cI_N$-Inv$_{ent}$380); lanes 6 and 7, JH372 pPD230 ($cI_N$-Inv$_{pstb}$575-694-Inv$_{ent}$380); lanes 8 and 9, JH372 pPD208 ($cI_N$-Inv$_{pstb}$478).

5-bromo-4-chloro-3-indolylphosphate (XP) and nitroblue tetrazolium (Boehringer) as substrates.

**ELISA to determine the invasin surface concentration.** Enzyme-linked immunosorbent assays (ELISAs) were used to compare the surface concentration of invasin in the outer membranes of $Y.$ $pseudotuberculosis$ and $Y.$ $enterocolitica$ cells. Serial dilutions of $2 \cdot 10^7$ bacteria were incubated in phosphate-buffered saline (PBS) containing 2% goat serum, 1 μg of primary anti-invasin antibodies (mAb3A2 for invasin$_{pstb}$ or a polyclonal invasin$_{ent}$ antiserum) per ml, followed by reprobing with 5 μg of goat anti-mouse or anti-rabbit immunoglobulin G alkaline phosphatase (Zymed) per ml for 1 h at room temperature. After washing, the cell density was redetermined at $A_{600}$ and the bacteria were incubated in AP-buffer with 1 mg of σ$^{104}$ alkaline phosphate substrate (Sigma) per ml in AP-buffer containing 100 mM Tris-HCl (pH 9.5), 5 mM MgCl$_2$, 150 mM NaCl$_2$. Exactly 20 min after starting the color reaction, the assay was monitored at 405 nm with a microtiter spectrophotometer (Bio-Rad). The amount of invasin on the bacterial cell surface was determined from standard ELISAs using the equivalent purified MBP-Invasin fusion protein. To do so, plastic wells were coated with serial dilutions of the purified fusion protein for 16 h at 4°C. The amount of bound protein was determined by subtracting the amount of protein that remained in the supernatant, determined by bicinchoninic acid protein assay. The relative amount of surface-exposed invasin concentration was determined by comparing the color reaction of the bacteria harboring invasin with that of the purified proteins, using concentrations that yielded a linear relationship between protein concentration and color reaction. Subsequently, the calculated invasin concentration was normalized to cell number. The corrected values shown (see Fig. 4C) are expressed relative to the amounts of surface-exposed invasin of uninduced bacteria XL1blue pPD207 ($inv_{pstb}$⁺), which is defined as 1.0.

**Cell binding and uptake assay.** In preparation for cell binding or uptake assays, $5 \times 10^4$ HEp-2 cells were seeded and grown overnight in individual wells of 24-well cell culture plates (Costar), using round coverslips when appropriate. Cell monolayers were washed three times with PBS and incubated in RPMI 1640 medium supplemented with 20 mM HEPES (pH 7.0) and 0.4% bovine serum albumin before the addition of approximately $5 \times 10^6$ bacteria. For the competitive invasion assays, equal amounts of $2.5 \times 10^6$ bacteria were premixed before addition to cells. Bacteria were centrifuged onto the cell monolayer (1,000 rpm, 5 min in a Hermle tabletop centrifuge) and incubated at 20°C to test for cell binding (and prevent bacterial uptake) or at 37°C to test for invasion. To assay cell binding, 1 h postinfection, the cells were washed three times with PBS and fixed with 2% paraformaldehyde in PBS for 20 min at room temperature. Subsequently, the samples were washed three times with PBS and mounted in PBS containing 0.1% p-phenylenediamine and 80% glycerol (vol/vol). Quantification of adherent bacteria was performed by using a Zeiss Axioskope (Jena, Germany). The total number of bacteria associated with the eukaryotic cell was determined by counting bacteria bound per HEp-2 cell under phase-contrast microscopy or with Giemsa-stained preparations. Two hundred individual cells were counted, and the number of adherent bacteria per cell was determined as the

mean of 50 individual cells. Bacterial uptake was assessed 90 min after infection as the percentage of bacteria which survived killing by the addition of the antibiotic gentamicin to the external medium, as described previously (7). For each strain, the relative level of bacterial uptake was determined by calculating the number of CFU that arose relative to the total number of bacteria introduced onto monolayers, performed in triplicate.

## RESULTS

The presence of D2 in the $Y.$ $pseudotuberculosis$ invasin protein and its absence in the $Y.$ $enterocolitica$ invasin suggested that these two proteins may differ in their relative abilities to either promote cellular uptake or undergo homotypic interaction (Fig. 1) (45). To further elucidate the role of the $Y.$ $pseudotuberculosis$ invasin D2 region, the ability of the invasin of $Y.$ $enterocolitica$ to mediate homotypic interaction was determined and the ability of the two homologs to promote bacterial uptake was compared.

**$Y.$ $enterocolitica$ invasin does not promote self-interaction in the one-hybrid assay.** In previous experiments, the region responsible for invasin$_{pstb}$-invasin$_{pstb}$ interaction was mapped to amino acids 595 to 694, which is now known to define the endpoints of D2 (7, 13) (Fig. 1A, dark blue domain). To investigate whether the $Y.$ $enterocolitica$ invasin is able to promote self-interaction, the monomeric DNA-binding domain of cI ($cI_N$) was fused to the C-terminal 380 amino acids of invasin$_{ent}$ ($cI_N$-Inv$_{ent}$380) and tested in the λ repressor one-hybrid assay. This hybrid is equivalent to $cI_N$-Inv$_{pstb}$478, in which the homologous domains of the C-terminus of invasin$_{pstb}$ were fused to $cI_N$. In addition, an $inv_{pstb}$ fragment carrying codons 575 to 694, which encompasses D2 (see Fig. 2 [7]), was inserted between $cI_N$ and the $inv_{ent}$ coding segment, to mimic invasin$_{pstb}$. The chimeric $cI_N$-Inv$_{ent}$ proteins were readily detected on SDS-polyacrylamide gels of cell extracts (Fig. 3) although the steady-state level of $cI_N$-Inv$_{pstb}$575-694-Inv$_{ent}$ was somewhat lower than that of the other chimerae (Fig. 3, lane 7).

The ability of the $cI_N$-Inv fusion proteins to repress transcription was tested, based on the property that only multi-

meric cI is able to form a repressor of the highest activity levels (13). As expected, a wild-type λ repressor, a $cI_N$-GCN4 chimera containing a leucine zipper dimerization domain, $cI_N$-$Inv_{pstb}$478, and $cI_N$-$Inv_{pstb}$575-694 yielded 84 to 99% repression of $\lambda P_R$, respectively (Fig. 2). In contrast, cells expressing the $cI_N$-$Inv_{ent}$380 protein yielded 52.4% repression of $\lambda P_R$, essentially identical to the monomeric $cI_N$ (41%) and $cI_N$-Inv202 proteins (48%), indicating that the construction containing the C terminus of $invasin_{ent}$ is monomeric. The triple hybrid $cI_N$-$Inv_{pstb}$575-694-$Inv_{ent}$380, which was less abundant in the cell compared to other fusion proteins, was still highly effective at repressing $\lambda P_R$ (99% repression; Fig. 2).

Strains expressing chimeric proteins that result in a functional dimeric or multimeric repressor, such as cI and cI-GCN4, confer immunity against the lytic phage λKH54 (ΔcI). In contrast, clones expressing monomeric cI proteins are sensitive to the phage (13). Consistent with previous results, the cI-$Inv_{pstb}$478 and cI-$Inv_{pstb}$596-694-$Inv_{ent}$380 proteins conferred resistance to the phage, implying multimer formation, while $cI_N$-$Inv_{ent}$380 failed to promote immunity to the phage (Fig. 2), consistent with its monomeric state.

**Invasin protein lacking D2 is defective for stimulation of uptake.** To determine if a lack of the D2 region has functional consequences on invasin-promoted uptake, two different internal in-frame deletion mutations removing the entire D2 region were introduced into the cloned $inv_{pstb}$ gene and placed into a low-copy-number vector under the control of the inducible *lacPO* promoter. The protein products differed in whether or not they had four *Y. enterocolitica* invasin residues (AVLP) that may provide a linker region in between two immunoglobulin superfamily domains [called (ΔD2)-1 and (ΔD2)-2; Fig. 1B]. Proteins with the expected molecular mass were detected in *E. coli* extracts for both $invasin_{pstb}$(ΔD2)-1 and $invasin_{pstb}$(ΔD2)-2, with expression levels that were similar to the $invasin_{pstb}$ and $invasin_{ent}$ proteins using the identical vector (data not shown). Invasin derivatives from both bacterial species and the two D2 deletion derivatives of $invasin_{pstb}$ were tested for binding to cultured cells (see Materials and Methods). In parallel, the efficiency of bacterial uptake was determined. To do so, *E. coli* cells expressing the different invasin derivatives were grown under conditions in which invasin expression was either highly induced (+IPTG) or uninduced (−IPTG). Binding to HEp-2 cells by *E. coli* derivatives harboring these constructions was essentially identical for each derivative, with about 4 ± 0.5 (mean ± standard deviation) bacteria associated per HEp-2 cell, in either the presence or absence of invasin overexpression (Fig. 4A). In the absence of induction, the ability of *E. coli* cells harboring the $invasin_{pstb}$ protein to enter HEp-2 cells was 10-fold higher than that of *E. coli* cells expressing the deletion derivatives or the $invasin_{ent}$ homologue (Fig. 4B). This result is in agreement with our previous observations in which a deletion of D2 and D3 (Fig. 1B) in the $invasin_{pstb}$ protein resulted in highly defective cellular entry of *Y. pseudotuberculosis* (7). When the inducer IPTG was added to the growth medium, invasin function increased, as judged by the amount of bacterial adhesion and uptake by HEp-2 cells (Fig. 4). The difference in uptake efficiencies promoted by $invasin_{pstb}$ relative to either $invasin_{ent}$ or the deletion derivatives was greatly reduced by induction. Under these conditions, uptake was 30 to 50% the level obtained with full-length $invasin_{pstb}$ (Fig. 4B). Thus, high production levels can compensate for the lower uptake efficiencies of the $Inv_{ent}$ and deletion proteins.

As uptake and adhesion strongly depended on the amount of protein expressed by the bacterium, differences in the uptake efficiencies of bacteria harboring the $inv_{ent}$ and $inv_{pstb}$
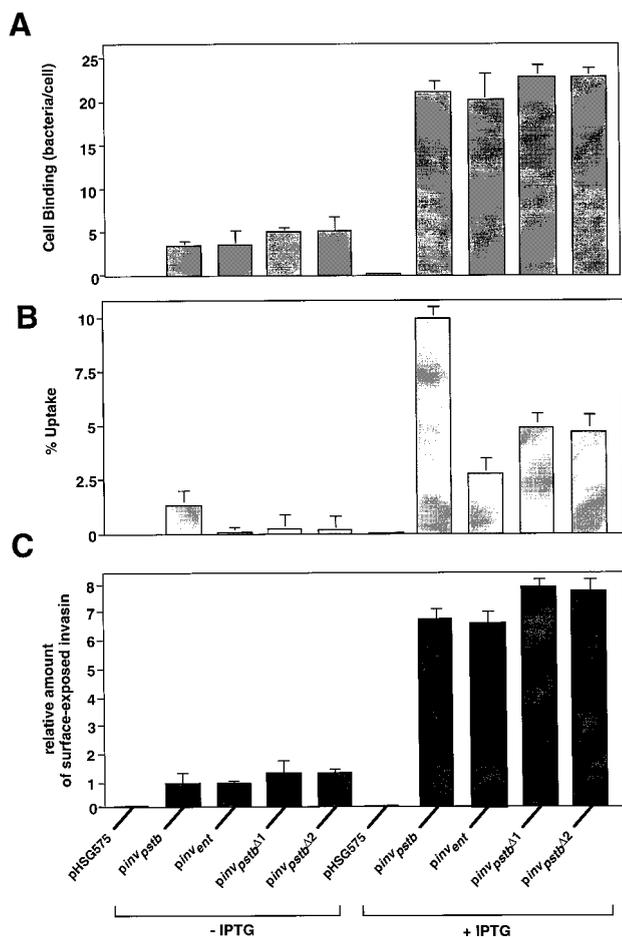
FIG. 4. Cell binding, entry efficiency, and surface exposure of different invasin alleles expressed by recombinant *E. coli* cells. *E. coli* XL1blue cells harboring plasmids pHSG575 (vector), pPD207 ($inv_{pstb}$), pPD231 ($inv_{ent}$), pPD254 ($inv_{pstb}$ΔD2-1), and pPD255 ($inv_{pstb}$ΔD2-2) were grown in M9 media with 0.4% glucose to an optical density at 600 nm of 0.7. Subsequently, the cultures were divided and grown for an additional 2 h in the presence or absence of 1 mM IPTG. An amount of $10^7$ bacteria was used to infect a HEp-2 cell monolayer of about $10^5$ cells to monitor their cell binding at 20°C and to determine invasion efficiency at 37°C (see Materials and Methods). The total number of cell-associated bacteria was visualized and counted microscopically (A), and the percentage internalized is shown (B). To compare the surface concentration of the invasin alleles on the bacterial cell surface, $2 \cdot 10^7$ bacteria were used for surface ELISAs probing with either monoclonal antibody mAb3A2 against $invasin_{pstb}$ or with a polyclonal antiserum against $invasin_{ent}$ (kindly provided by V. Miller). Identical ELISAs performed in parallel with plastic wells coated with purified MBP-$Inv_{ent}$ and MBP-$Inv_{pstb}$ proteins were used to standardize the color reaction and determine the number of invasin molecules in the bacterial outer membrane. The values shown are expressed relative to the amounts of surface-exposed invasin of bacteria XL1blue pPD207 ($inv_{pstb}^+$) without IPTG, defined as 1.0 (C).

genes could result from either differing protein expression levels or export efficiencies. To examine whether the different derivatives were exported equally to the outer membrane, a surface ELISA technique was performed to determine the number of surface-exposed invasin molecules in the bacterial outer membrane. *E. coli* cells harboring the invasin derivatives were grown under the same conditions used for the cell binding and invasion assays, and the amount of invasin on the bacterial cell surface was quantified (see Materials and Methods). Similar numbers of the $Inv_{ent}$ and the $Inv_{pstb}$ proteins were found in the outer membranes of *E. coli* cells, although the amount of surface-localized protein was approximately 10% higher for
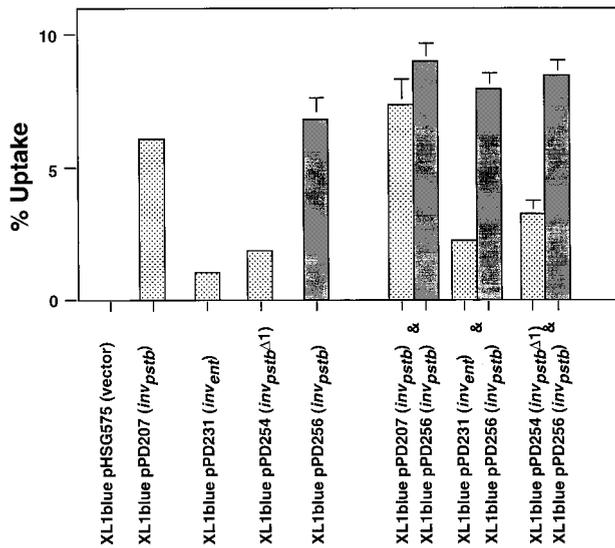
FIG. 5. Competitive uptake assays using two recombinant *E. coli* strains expressing either wild-type invasin*pstb* or another invasin derivative. *E. coli* XL1blue cells harboring plasmids pHSG575 (vector), pPD207 (*inv*$_{pstb}$), pPD231 (*inv*$_{ent}$), pPD254 (*inv*$_{pstb}$ΔD2-1), and pPD256 (*inv*$_{pstb}$) were grown in M9 media with 0.4% glucose to an optical density at 600 nm of 0.7. Subsequently, the cultures were grown for additional 2 h under inducing conditions with 2 mM IPTG. For the competition experiment, equal amounts of XL1blue pPD256 and XL1blue cells harboring either pPD207, pPD254, or pPD231 were mixed and $10^7$ bacteria were used to infect a HEp-2 cell monolayer of about $10^5$ cells at 37°C (for details see Materials and Methods). The percentage of single or mixed bacteria internalized is shown. Error bars represent the standard deviations of the means of four groups of 50 cells counted in various regions of the stained specimens, and data presented are one of three typical independent experiments.

the deletion derivatives (Fig. 4C). This relationship between derivatives was maintained in either the presence or absence of the inducer IPTG (Fig. 4C). Hence, the differences in the uptake efficiencies of the invasin homologs must be explained by the distinct properties of these proteins and not by differences in expression or presentation of proteins on the bacterial cell surface.

**Inefficient competition by overexpressed invasin derivatives lacking D2.** To examine if, under conditions of overproduction, bacteria harboring *inv*$_{pstb}$ are indeed more efficient at promoting uptake than bacteria harboring *inv*$_{ent}$, competitive uptake experiments were performed. An ampicillin resistance cassette was inserted into the chloramphenicol resistance gene of pPD207 (*inv*$_{pstb}^+$) to distinguish between *E. coli* strains expressing the invasin*pstb* wild type or the deleted invasin alleles. Subsequently HEp-2 cells were coinfected with either equal amounts of recombinant *E. coli* XL1blue pPD256 (*inv*$_{pstb}^+$) and XL1blue pPD231 (*inv*$_{ent}^+$) or XL1blue pPD254 (*inv*$_{pstb}$ (ΔD2)-1) after growing the strains under inducing conditions (+IPTG). The uptake efficiencies of the deletion derivatives were less than 40% that of the wild type (Fig. 5). This parallels the results of experiments using HEp-2 cells challenged with single bacterial strains. Therefore, even under conditions that maximize expression of the deletion derivatives, the proteins lacking D2 were less active than invasin*pstb*.

## DISCUSSION

This study demonstrated that in contrast to *Y. pseudotuberculosis*, the invasin protein of *Y. enterocolitica* which lacks the self-association domain D2 was not capable of promoting homotypic interaction. This result was also supported by in vivo

cross-linking experiments, in which efficient cross-linking of high-molecular-weight complexes of invasin could only be seen with invasin*pstb* but not with derivatives lacking D2 (data not shown). To examine if the lowered efficiency of invasin*ent* multimer formation affected its function, we compared cell attachment and uptake mediated by the invasins from these two *Yersinia* species or to in-frame deletions of invasin*pstb* engineered to resemble the natural deletion in invasin*ent*. In all cases, *E. coli* cells carrying the invasin*pstb* clone were significantly more proficient at uptake than *E. coli* expressing the deletion derivatives, although high-level expression of derivatives lacking D2 significantly overcame this difference. Therefore, we conclude that D2 is a critical determinant for promoting uptake under conditions in which invasin concentration is limiting.

Functional differences between the *Y. pseudotuberculosis* and *Y. enterocolitica* invasin have been observed previously (28, 45). Miller and coworkers found that the uptake efficiency of *inv*$_{ent}$-harboring strains was 6- to 60-fold lower than that of *inv*$_{pstb}$ strains, depending on the cell line being analyzed. The results obtained here are also consistent with a previous analysis of D2 (7), in which far more internalization was observed with beads coated by an invasin derivative containing D1 to D5 than by D4 and D5 alone. Thus, lack of multivalency seems to strongly correlate with a decrease in the ability to be internalized by mammalian cells. This result emphasizes the importance of invasin-invasin interaction for efficient internalization.

We propose that interaction of homomultimeric invasin with multiple integrin receptors establishes intimate adherence and receptor clustering, providing a signal for internalization. It has been shown that the interaction of extracellular matrix proteins with $\beta_1$ integrins leads to the association of multiple signaling proteins and cytoskeletal elements at the site of binding to substrate (43). The invasin-bound integrin complex is still uncharacterized, although it appears to consist of several tyrosine-phosphorylated proteins, such as Paxillin, Cas$^{130}$, and FAK (1; P. Dersch, unpublished results). As monomeric and multimeric forms of invasin lead to different cellular responses (7), there may be differences in the signaling molecules associated with the integrin after adherence with each form. Furthermore, the concentrations of signaling proteins recruited to the cytoplasmic domain of $\beta_1$ integrins may depend on the multimerization state of the protein, affecting relative uptake efficiencies.

The relative efficiency of bacterial uptake mediated by different invasin alleles strongly depends on the amount of surface-localized invasin molecules (see Fig. 4C). Under noninducing conditions, under which a small number of invasin*pstb* molecules was expressed on the surface of *E. coli* cells, uptake was approximately 6- to 10-fold higher than uptake of bacteria having invasin derivatives lacking D2. High expression levels, however, greatly suppressed this difference in uptake efficiency, allowing compensation for the absence of D2. This finding agrees well with previous observations using invasin-coated latex beads, in which invasin*pstb* having only D4 and D5 (Fig. 1A) required more than 10,000 molecules per bead to promote efficient uptake (7). This coating concentration is approximately 10 times higher than that necessary to promote uptake by D1 to D5.

It is unclear what pressures resulted in *Y. enterocolitica* and *Y. pseudotuberculosis* having invasin molecules with different numbers of immunoglobulin superfamily repeat modules. In addition to invasin, differences between adhesion proteins of *Y. enterocolitica* and *Y. pseudotuberculosis* have been observed. *Y. enterocolitica* Ail was first identified as a protein that mediates cell adhesion and low-level uptake (29). In contrast, the *Y.*

*pseudotuberculosis* Ail protein promotes neither cell binding nor cell entry (44). Furthermore, the plasmid-encoded adhesion factor YadA of *Y. enterocolitica* seems to be more efficient in tissue culture uptake experiments than its *Y. pseudotuberculosis* homologue and has been demonstrated to play a more critical role in *Y. enterocolitica* virulence than that observed with *Y. pseudotuberculosis* (34). Thus, it seems very likely that although the *Y. enterocolitica* invasin is less competent at promoting uptake than invasin$_{pstb}$, this has been compensated for by features in proteins such as Ail and YadA that allow them to be more effective at cellular interaction than their *Y. pseudotuberculosis* counterparts. It is likely that these differences have consequences on the relative courses of infection taken by these two species. *Yersinia* species have fairly broad host ranges and a particular adhesion factor may be more effective in one animal host than in another. A second explanation for differences in activities of similar proteins is that the two bacterial species may use the identical adhesive factors for different purposes. Perhaps even the tissue site of action of a particular adhesin differs between the two bacterial species.

Slight alterations in invasin function may explain differences in the colonization pattern of the enteropathogenic *Yersinia* species and may also be responsible for their distinct pathogenicities. Both *Y. enterocolitica* and *Y. pseudotuberculosis* translocate through the intestinal epithelial layer via M cells overlaying the Peyer's patches. Subsequent colonization of the underlying lymphatic tissue seems to be significantly different, and may be altered by relative invasin function. It has been observed that *Y. enterocolitica* cells form abscesses associated with large numbers of bacteria in the mouse Peyer's patch, while infections with *Y. pseudotuberculosis* yield much smaller numbers of bacteria with no abscesses in this site (Ingo Authenrieth, personal communication; P. Barnes and R. Isberg, unpublished results). It is possible that the increased activity of invasin$_{pstb}$ may allow more efficient bypass of antiphagocytosis promoted by YopH and YopE, with the consequence of reducing the proliferation of *Y. pseudotuberculosis* within lymph nodes. Future analysis of animal infection models is needed to fully evaluate the consequences of differences in the properties of adhesive protein encoded by enteropathogenic *Yersinia* species.

## REFERENCES

1. **Alrutz, M. A., and R. R. Isberg.** 1998. Involvement of focal adhesion kinase in invasin-mediated uptake. Proc. Natl. Acad. Sci. USA **95:**13658–13663.
2. **Altschul, S. F., W. Gish, W. Miller, E. W. Myers, and D. J. Lipman.** 1990. Basic local alignment search tool. J. Mol. Biol. **215:**403–410.
3. **Bliska, J. B., M. C. Copass, and S. Falkow.** 1993. The *Yersinia pseudotuberculosis* adhesin YadA mediates intimate bacterial attachment to and entry into HEp-2 cells. Infect. Immun. **61:**3914–3921.
4. **Bolin, I., I. Norlander, and H. Wolf-Watz.** 1982. Temperature-inducible outer membrane protein of *Yersinia pseudotuberculosis* and *Yersinia enterocolitica* is associated with the virulence plasmid. Infect. Immun. **37:**506–512.
5. **Bolivar, F., R. L. Rodriguez, P. J. Greene, M. C. Betlach, H. L. Heyneker, and H. W. Boyer.** 1977. Construction and characterization of new cloning vehicles. II. A multipurpose cloning system. Gene **2:**95–113.
6. **Bullock, W. O., J. M. Fernandez, and J. M. Short.** 1987. XL1-Blue: a high efficiency plasmid transforming *recA Escherichia coli* strain with beta-galactosidase selection. T. Biotechniques **5:**376–379.
7. **Dersch, P., and R. R. Isberg.** 1999. A region of the *Yersinia pseudotuberculosis* invasin protein enhances integrin-mediated uptake into mammalian cells and promotes self-association. EMBO J. **18:**1199–1213.
8. **Finlay, B. B., and S. Falkow.** 1997. Common themes in microbial pathogenicity revisited. Microbiol. Mol. Biol. Rev. **61:**136–169.
9. **Finlay, B. B., and S. Falkow.** 1988. Comparison of the invasion strategies used by *Salmonella cholerae-suis, Shigella flexneri* and *Yersinia enterocolitica* to enter cultured animal cells: endosome acidification is not required for bacterial invasion or intracellular replication. Biochimie **70:**1089–1099.
10. **Frankel, G., D. C. Candy, P. Everest, and G. Dougan.** 1994. Characterization of the C-terminal domains of intimin-like proteins of enteropathogenic and enterohemorrhagic *Escherichia coli, Citrobacter freundii,* and *Hafnia alvei.* Infect. Immun. **62:**1835–1842.
11. **Grutzkau, A., C. Hanski, H. Hahn, and E. O. Riecken.** 1990. Involvement of M cells in the bacterial invasion of Peyer's patches: a common mechanism shared by *Yersinia enterocolitica* and other enteroinvasive bacteria. Gut **31:**1011–1015.
12. **Hamburger, Z. A., M. S. Brown, R. R. Isberg, and P. J. Bjorkman.** 1999. Crystal structure of invasin: a bacterial integrin-binding protein. Science **286:**291–295.
13. **Hu, J. C., E. K. O'Shea, P. S. Kim, and R. T. Sauer.** 1990. Sequence requirements for coiled-coils: analysis with lambda repressor- GCN4 leucine zipper fusions. Science **250:**1400–1403.
14. **Hynes, R. O.** 1992. Integrins: versatility, modulation, and signaling in cell adhesion. Cell **69:**11–25.
15. **Isberg, R. R.** 1991. Discrimination between intracellular uptake and surface adhesion of bacterial pathogens. Science **252:**934–938.
16. **Isberg, R. R.** 1990. Pathways for the penetration of enteroinvasive *Yersinia* into mammalian cells. Mol. Biol. Med. **7:**73–82.
17. **Isberg, R. R., and J. M. Leong.** 1988. Cultured mammalian cells attach to the invasin protein of *Yersinia pseudotuberculosis.* Proc. Natl. Acad. Sci. USA **85:**6682–6686.
18. **Isberg, R. R., A. Swain, and S. Falkow.** 1988. Analysis of expression and thermoregulation of the *Yersinia pseudotuberculosis inv* gene with hybrid proteins. Infect. Immun. **56:**2133–2138.
19. **Isberg, R. R., D. L. Voorhis, and S. Falkow.** 1987. Identification of invasin: a protein that allows enteric bacteria to penetrate cultured mammalian cells. Cell **50:**769–778.
20. **Jerse, A. E., J. Yu, B. D. Tall, and J. B. Kaper.** 1990. A genetic locus of enteropathogenic *Escherichia coli* necessary for the production of attaching and effacing lesions on tissue culture cells. Proc. Natl. Acad. Sci. USA **87:**7839–7843.
21. **Kelly, G., S. Prasannan, S. Daniell, K. Fleming, G. Frankel, G. Dougan, I. Connerton, and S. Matthews.** 1999. Structure of the cell-adhesion fragment of intimin from enteropathogenic *Escherichia coli.* Nat. Struct. Biol. **6:**313–318.
22. **Leong, J. M., R. S. Fournier, and R. R. Isberg.** 1990. Identification of the integrin binding domain of the *Yersinia pseudotuberculosis* invasin protein. EMBO J. **9:**1979–1989.
23. **Leong, J. M., R. S. Fournier, and R. R. Isberg.** 1991. Mapping and topographic localization of epitopes of the *Yersinia pseudotuberculosis* invasin protein. Infect. Immun. **59:**3424–3433.
24. **Leong, J. M., P. E. Morrissey, A. Marra, and R. R. Isberg.** 1995. An aspartate residue of the *Yersinia pseudotuberculosis* invasin protein that is critical for integrin binding. EMBO J. **14:**422–431.
25. **Marra, A., and R. R. Isberg.** 1997. Invasin-dependent and invasin-independent pathways for translocation of *Yersinia pseudotuberculosis* across the Peyer's patch intestinal epithelium. Infect. Immun. **65:**3412–3421.
26. **McGraw, E. A., J. Li, R. K. Selander, and T. S. Whittam.** 1999. Molecular evolution and mosaic structure of alpha, beta, and gamma intimins of pathogenic *Escherichia coli.* Mol. Biol. Evol. **16:**12–22.
27. **Miller, J. H.** 1992. A short course in bacterial genetics: a laboratory manual and handbook for *Escherichia coli* and related bacteria. Cold Spring Harbor Laboratory, Cold Spring Harbor, N.Y.
28. **Miller, V. L.** 1992. *Yersinia* invasion genes and their products. ASM News **58:**26–32.
29. **Miller, V. L., and S. Falkow.** 1988. Evidence for two genetic loci in *Yersinia enterocolitica* that can promote invasion of epithelial cells. Infect. Immun. **56:**1242–1248.
30. **Moulder, J. W.** 1985. Comparative biology of intracellular parasitism. Microbiol. Rev. **49:**298–337.
31. **Neutra, M. R., N. J. Mantis, A. Frey, and P. J. Giannasca.** 1999. The composition and function of M cell apical membranes: implications for microbial pathogenesis. Semin. Immunol. **11:**171–181.
32. **Pepe, J. C., J. L. Badger, and V. L. Miller.** 1994. Growth phase and low pH affect the thermal regulation of the Yersinia enterocolitica inv gene. Mol. Microbiol. **11:**123–135.
33. **Pepe, J. C., and V. L. Miller.** 1993. *Yersinia enterocolitica* invasin: a primary role in the initiation of infection. Proc. Natl. Acad. Sci. USA **90:**6473–6477.
34. **Pepe, J. C., M. R. Wachtel, E. Wagar, and V. L. Miller.** 1995. Pathogenesis of defined invasion mutants of *Yersinia enterocolitica* in a BALB/c mouse model of infection. Infect. Immun. **63:**4837–4848.
35. **Rankin, S., R. R. Isberg, and J. M. Leong.** 1992. The integrin-binding domain

of invasin is sufficient to allow bacterial entry into mammalian cells. Infect. Immun. **60:**3909–3912.

36. **Rosenshine, I., V. Duronio, and B. B. Finlay.** 1992. Tyrosine protein kinase inhibitors block invasin-promoted bacterial uptake by epithelial cells. Infect. Immun. **60:**2211–2217.

37. **Saltman, L. H., Y. Lu, E. M. Zaharias, and R. R. Isberg.** 1996. A region of the *Yersinia pseudotuberculosis* invasin protein that contributes to high affinity binding to integrin receptors. J. Biol. Chem. **271:**23438–23444.

38. **Sambrook, J., E. F. Fritsch, and T. Maniatis.** 1989. Molecular cloning: a laboratory manual. Cold Spring Harbor Laboratory, Cold Spring Harbor, N.Y.

39. **Schauer, D. B., and S. Falkow.** 1993. The *eae* gene of *Citrobacter freundii* biotype 4280 is necessary for colonization in transmissible murine colonic hyperplasia. Infect. Immun. **61:**4654–4661.

40. **Takeshita, S., M. Sato, M. Tabo, W. Masahashi, and T. Hashimoto-Gothoh.** 1987. High-copy-number and low-copy-number plasmid vectors for *lacZ*

α-complementation and chloramphenicol- or kanamycin resistance selection. Gene **61:**63–74.

41. **Tran Van Nhieu, G., E. S. Krukonis, A. A. Reszka, A. F. Horwitz, and R. R. Isberg.** 1996. Mutations in the cytoplasmic domain of the integrin beta1 chain indicate a role for endocytosis factors in bacterial internalization. J. Biol. Chem. **271:**7665–7672.

42. **Weis, W. I., M. E. Taylor, and K. Drickamer.** 1998. The C-type lectin superfamily in the immune system. Immunol. Rev. **163:**19–34.

43. **Yamada, K. M., and S. Miyamoto.** 1995. Integrin transmembrane signaling and cytoskeletal control. Curr. Opin. Cell Biol. **7:**681–689.

44. **Yang, Y., J. J. Merriam, J. P. Mueller, and R. R. Isberg.** 1996. The *psa* locus is responsible for thermoinducible binding of *Yersinia pseudotuberculosis* to cultured cells. Infect. Immun. **64:**2483–2489.

45. **Young, V. B., V. L. Miller, S. Falkow, and G. K. Schoolnik.** 1990. Sequence, localization and function of the invasin protein of *Yersinia enterocolitica*. Mol. Microbiol. **4:**1119–1128.

*Editor:* J. D. Clements